Published in final edited form as:
Microvasc Res. 2011 January ; 81(1): 44–51. doi:10.1016/j.mvr.2010.10.003.

Support of a Free Radical Mechanism for Enhanced Antitumor Efficacy of the Microtubule Disruptor OXi4503

Lori Rice[1,*], **Christine Pampo**[1], **Sharon Lepler**[1], **Amyn M Rojiani**[2], and **Dietmar W. Siemann**[1]

[1]Department of Radiation Oncology, University of Florida, Gainesville, FL, USA

[2]Department of Pathology, Medical College of Georgia, Augusta, GA, USA

Abstract

Unlike normal blood vessels, the unique characteristics of an expanding, disorganized and leaky tumor vascular network can be targeted for therapeutic gain by vascular disrupting agents (VDAs), which promote rapid and selective collapse of tumor vessels, causing extensive secondary cancer cell death. A hallmark observation following VDA treatment is the survival of neoplastic cells at the tumor periphery. However, comparative studies with the second generation tubulin-binding VDA OXi4503 indicate that the viable rim of tumor tissue remaining following treatment with this agent is significantly smaller than that seen for the lead VDA, combretastatin. OXi4503 is the cis-isomer of CA1P and it has been speculated that this agent's increased antitumor efficacy may be due to its reported metabolism to orthoquinone intermediates leading to the formation of cytotoxic free radicals. To examine this possibility in situ, KHT sarcoma-bearing mice were treated with either the cis- or trans-isomer of CA1P. Since both isomers can form quinone intermediates but only the cis-isomer binds tubulin, such a comparison allows the effects of vascular collapse to be evaluated independently from those caused by the reactive hydroxyl groups. The results showed that the cis-isomer (OXi4503) significantly impaired tumor blood flow leading to secondary tumor cell death and >95% tumor necrosis 24 h post drug exposure. Treatment with the trans-isomer had no effect on these parameters. However, the combination of the trans-isomer with combretastatin increased the antitumor efficacy of the latter agent to near that of OXi4503. These findings indicate that while the predominant in vivo effect of OXi4503 is clearly due to microtubule collapse and vascular shut-down, the formation of toxic free radicals likely contributes to its enhanced potency.

Keywords

OXi4503; combretastatin; vascular disrupting agents; endothelial cells; magnetic resonance imaging; viable rim; tubulin-binding agents

[*]Corresponding author: Lori Rice, PhD, Department of Radiation Oncology, University of Florida, 2033 Mowry Rd. 485E, Gainesville, FL 32610, USA, Tel: 352-273-8262, Fax: 352-273-8252, lrice@ufl.edu.

Introduction

Neoplasms larger than a few millimeters in size require an extensive blood supply to support their growing mass (Horsman and Siemann, 2006). The resultant neovasculature is abnormal in both structure and function, exhibiting disorganized vessels with irregular, chaotic, and often leaky branches, lack of normal smooth muscle and pericyte components, incomplete basement membranes, and thin walls (Chan et al., 2008a; Davis et al., 2002; Sheng et al., 2004; Siemann et al., 2004). Another critical feature of tumor vasculature is its active proliferative state (Azam et al., 2010; Bloemendal et al., 1999; Denekamp, 1982, 1999; Denekamp and Hobson, 1982; Hobson and Denekamp, 1984; Ljungkvist et al., 2002). The latter makes it vulnerable to small molecule microtubule-disrupting agents, such as the combretastatins, a family of compounds originally derived from the *Combretum caffrum* tree, that selectively inhibit tubulin polymerization in proliferating endothelial cells (Galbraith et al., 2001; Grosios et al., 1999; Hamel and Lin, 1983; Lin et al., 1988; Vincent et al., 2005). The observed vulnerability of dividing endothelial cells led to their extensive evaluation in a variety of rodent and human tumor models (Holwell et al., 2002; Malconenti-Wilson et al., 2001; Salmon and Siemann, 2006; Thorpe, 2004). A recent, detailed review of tumor effects by the combretastatins and others of this class, subsequently termed vascular disrupting agents (VDAs), can be found elsewhere (Siemann, 2010). Briefly, in vivo findings that VDAs promote rapid and selective shutdown of tumor blood flow (Chaplin et al., 2006; Gaya and Rustin, 2005; Lippert, 2007; Siemann and Horsman, 2004; Siemann et al., 2005) and extensive secondary cancer cell death (Chan et al., 2007; Kirwan et al., 2004; Shnyder et al., 2003; Siemann et al., 2002) provided the impetus for their introduction into clinical trials (Beerepoot et al., 2006; Dowlati et al., 2002; Rossi et al., 2009; Rustin et al., 2003; Siemann et al., 2009).

The lead combretastatin, CA4P (combretastatin-A4 phosphate, Zybrestat ™), and its second generation analog, CA1P (OXi4503), have been shown to reversibly bind tubulin at the colchicine binding site (Calligaris et al., 2010; Sriram, et.al., 2008; Lippert, et al., 2007) and to potently disrupt polymerization of tubulin molecules (Bijman et al., 2006; Kanthou and Tozer, 2009; McKeage and Baguley, 2010). In vivo CA4P and OXi4503 treatments induce significant blood flow reductions and extensive necrosis in a wide variety of preclinical cancer models (Hill et al., 2002; Malcontenti-Wilson et al., 2001; Salmon and Siemann, 2006; Salmon et al., 2006). However, there is a growing body of evidence that suggests that the latter agent may be more potent (Folkes et al., 2007; Holwell et al., 2002; Horsman and Siemann, 2006; Salmon and Siemann, 2006; Thorpe, 2004) Treatment with either agent results in widespread central necrosis, but the surviving viable rim at the tumor periphery, a common observation for all VDAs, (Chan et al., 2008b; Rojiani and Rojiani, 2006; Salmon et al., 2006; Siemann and Horsman, 2009), has been noted to be much smaller following treatment with OXi4503 (Hua et al., 2003; Rojiani and Rojiani, 2006; Thorpe, 2004). Measures of tumor perfusion showed that both CA4P and OXi4503 caused maximal vessel shutdown by 4 h post-treatment, but magnetic resonance imaging (MRI) revealed that blood flow remained low for a longer period of time in OXi4503-treated tumors than with CA4P (Salmon and Siemann, 2006). In addition, whereas CA4P treatment rarely impacts tumor growth, OXi4503 exposure can induce significant tumor growth delays (Hill et al., 2002; Holwell et al., 2002; Hua et al., 2003; Salmon and Siemann, 2006).

Although the chemical structures of the de-phosphorylated active forms of these agents differ only in the addition of a hydroxyl group to OXi4503 (Folkes et al., 2007), speculation has centered on the possibility that chemical activation confers greater potency to this compound due to direct cytotoxic effects (Hill et al., 2002). Investigations into this possibility have identified the formation of reactive orthoquinones that bind to cellular nucleophiles and form free radicals (Folkes et al., 2007; Lippert, 2007). Chemical oxidation

reactions to observe free radical formation and redox properties of the two agents showed that oxidation of OXi4503 allowed the formation of a metabolite with an additional phenolic moiety, with orthoquinones as key intermediates (Folkes et al., 2007). Studies in mice subsequently confirmed that the intermediates were capable of reacting with both proteins and nucleic acids, consistent with known cytotoxic effects of quinones (Folkes et al., 2007).

The goal of the present investigations was to gain a better perspective of the potential role of the quinone moieties in the in vivo mechanisms of action of OXi4503 by comparing the action of OXi4503 (the *cis*-isomer of CA1P) with that of the *trans*-isomers of CA1P. Since *trans*-CA1P lacks tubulin-binding activity, possible antitumor effects solely due to the reactive hydroxyl groups could be evaluated independently from those resulting from vascular collapse.

Materials and Methods

Cell Lines and Animal Models

Human microvascular endothelial cells (HMVEC-L, Lonza Biologics, Walkersville, MD) were maintained in EGm2-mv media (Lonza) in a humidified 5% CO_2 incubator at 37°C.

KHT sarcoma cells (Kallman et al., 1967) were maintained by in vivo passage. At passage, harvested tumors were dissociated and 10^5 cells injected intramuscularly into the hind limb of female C3H/HeJ mice, aged 4-6 weeks (Fredrick Cancer Research Facility, Fredrick, MD). Mice were housed in facilities approved by the American Association for Accreditation of Laboratory Animal Care, and supplied with food and water ad libitum. All experiments involving these mice were performed according to the guidelines of the Institutional Animal Care and Use Committee of the University of Florida.

Drugs

Cis-CA1P (OXi4503) and *trans*-CA1P were kindly provided by OXiGENE (Waltham, MA) and prepared in sterile saline containing 0.25% sodium carbonate per milliliter, for administration by intraperitoneal injection in mice or for addition to cell culture media.

Endothelial Cell Tube Assays

Tube Formation—To assess tube formation, HMVEC-L cells (6×10^4) were pre-treated with either OXi4503 or *trans*-CA1P at a concentrations from 10 nM to 10 μM, for 30 min or 4 h, then placed in fresh media and plated on a basement membrane matrix (Matrigel®, BD Biosciences, Palo Alto, CA) in 24-well plates. Tube formation was assessed by light microscopy 4 h and 24 h after plating.

To assess tube disruption, HMVEC-L cells (6×10^4) were placed in 24-well plates on Matrigel and allowed to form tubes for 18 h. Then, they were exposed to OXi4503 or *trans*-CA1P at a concentration of 10 μM for 30 min or 4 h. The agents were then removed and replaced with fresh media. Tube status was evaluated 24 h after treatment.

Tubulin Depolymerization

HMVEC-L cells (10^4) were plated on 2-well chamber slides and allowed to adhere overnight. The cells were then exposed to either OXi4503 or *trans*-CA1P at a concentration of 10 μM for either 30 min or 4 h. Following the incubation period, the cells were fixed and immunostained with antibodies to β-actin (conjugated to Cy3) and β-tubulin (conjugated to Cy2) (Sigma, St. Louis, MO). Nuclear DNA was counterstained with DAPI. Microtubule structure was assessed by confocal microscopy.

Clonogenic Cell Survival

Survival of cells derived from solid tumors was determined as previously described (Salmon and Siemann, 2006). Briefly, mice bearing KHT sarcomas were treated with various doses (0-25 mg/kg) of either OXi4503 or *trans*-CA1P. Twenty-four hours later, the tumors were removed, dissociated, and single cells were plated in various dilutions in 24-well plates. After 2 weeks of incubation, colonies of greater than 50 cells were counted. Surviving fraction was calculated as the percent of plated cells that formed colonies in treated dishes compared to control. The tumor surviving fraction was determined by correcting for the percent of viable cells harvested per gram of tumor in treated tumors compared to controls.

Morphologic and Morphometric Analysis of Tumor Histology

KHT tumors were dissected from the hind limbs of mice 24 h after treatment with CA4P, OXi4503, *trans*-CA1P, or a combination of CA4P plus the *trans*-isomer. Following overnight fixation in 10% buffered formalin, each tumor was inked around the entire surface to define the borders. Tumors were serially dehydrated in graded alcohols, processed in xylene and embedded in paraffin. Four-micron sections were cut and stained with hematoxylin and eosin, as well as Masson's trichrome stain. Alternate slices were submitted for routine histology. For determination of morphology, each section was divided into 4-8 grids using a fine permanent marker. Images were viewed and captured using a Zeiss Zxiophot 2 microscope (Carl Zeiss Jena GmbH, Jena Germany) with Sony DXC970 color camera (Sony Corporation, Tokyo, Japan), then assessed with an Image Pro Plus image analysis system (Media Cybernetics, Silver Spring, MD). Using an “irregular area of interest” tool, areas of necrosis were outlined and measured on each grid. Multiple grids for each tumor were reconstructed by tiled field mapping and the necrotic area was compared with the total area of the tumor using a MCID5.5 image analysis program (Imaging Research Inc., Ontario, Canada), as described previously (Rojiani et al., 2002). Areas of tumor necrosis were identified from the hyperchromatic, pleomorphic, mitotically active viable tumor cells. The tumor necrotic fraction was then calculated using the formula: % Tumor Necrosis = Necrotic Tumor Area/Total Tumor Area × 100% (Rojiani and Rojiani, 2006; Salmon et al 2006; Siemann and Rojiani, 2005) with the aid of the Image J software program (National Health Institute, Bethesda, MD). A board certified pathologist (AR), who was blinded to the sample identity, evaluated the tissue sections for histomorphology and percent tumor necrosis.

Patent Tumor Blood Vessels

Quantification of patent blood vessels in KHT tumors was performed using a Chalkley point array for random sample analysis as described previously (Salmon and Siemann, 2006; Salmon and Siemann, 2007). Briefly, at various times after treatment with either OXi4503 or *trans*-CA1P (25 mg/kg), mice were intravenously administered 40 mg/kg of a Hoechst-33342 (bisbenzimide, Sigma) solution prepared in sterile saline immediately before use. One minute after injection of Hoechst-33342, the mice were euthanized. The tumors were then excised and flash frozen in liquid nitrogen. Subsequently, 10-micron sections were prepared for vessel counts, cut at 3 different levels between one pole and the equatorial plane. The sections were air dried and then viewed under UV light using a fluorescent microscope. Blood vessel outlines were identified by the surrounding halo of fluorescent Hoechst-33342-labeled cells. Vessel counts were performed using a Chalkley point array for random sample analysis (Hansen, et al., 2000). As described previously, a 25-point Chalkley grid was positioned randomly over a field of view. Any points falling within haloes of fluorescent cells were scored as positive (Salmon, et al., 2006; Siemann and Rojiani, 2002; Siemann and Rojiani, 2005). For each tumor, the mean vessel density was determined on 20 random fields from 10 tumor sections, with 3-5 tumors evaluated per group.

Tumor Perfusion

Tumor perfusion in mice bearing KHT sarcomas was determined using dynamic contrast enhanced magnetic resonance imaging (DCE-MRI) as previously described (Salmon and Siemann, 2006). Briefly, scans were made of each mouse before and 4 and 24 h after administration of a single dose of either OXi4503 or *trans*-CA1P (25 mg/kg), using the contrast agent gadolinium-diethylenetriaminepentaacetic acid (GdDTPA, Omniscan, GE Healthcare, London, UK). Contrast-enhanced MR images were acquired using a 4.7-Tesla horizontal bore magnet (Oxford Instruments, Oxfordshire, UK), for a period of 15 min after administration of GdDTPA. Tumor perfusion at each time point was quantified by plotting the mean tumor pixel signal intensity over time, after injection of the contrast agent, and integrating the area under the signal intensity-time curve using the MAS software program, which normalizes for pre-GdDTPA signal.

Results

Efficacy of VDAs in solid tumors is the consequence of vascular damage leading to secondary tumor cell death due to ischemia (Siemann and Horsman, 2009). Tumors of mice treated with OXi4503 (25 mg/kg) revealed a rapid loss of patent blood vessels as assessed by Hoechst-33342 staining (Fig. 1). A reduction in the tumor blood vessel network became apparent within 30 min of treatment, reaching a nadir at 4 h. Even 24 and 48 h post-treatment, the average numbers of vessels per high power field remained significantly lower than those in untreated control tumors. In contrast, treatment with the *trans*- isomer did not significantly affect the number of patent tumor blood vessels over the entire time period evaluated.

In vitro, human microvascular endothelial cells (HMVEC-L), evaluated by immunofluorescence microscopy following treatment with OXi4503, illustrated progressively adverse microtubule structural changes that were readily apparent within 30 min post-treatment (Fig. 2). Actin and tubulin lost the filamentous shape seen in control cells and the cells became rounder. Evidence of even greater tubulin destabilization was seen by 4 h post-drug exposure. In contrast, endothelial cells exposed to the *trans*-CA1P isomer for the same treatment period showed little damage and appeared indistinguishable from control cells.

Endothelial cells that were exposed to various concentrations of OXi4503 (10 nM to 10 μM) for 30 min prior to plating on Matrigel, produced early-stage tubes, similar to those in the control group at 4 h post-plating, although at 10 μM, the tubes were slightly less organized (Fig. 3a). However, by 24 h post-plating, cells in the 10 μM treatment group were not only unable to complete the tube formation process, the partially completed structures seen at 4 h were disrupted. In contrast, cells pretreated with up to 10 μM *trans*-CA1P for 30 min produced tube networks indistinguishable from controls (Fig. 3a). When endothelial cells were pretreated with OXi4503 for 4 h and then assessed at 4 h post-plating, the results were similar to those observed after 30 min drug exposure in that only the cells treated with 10 μM had less organized tubes than the controls (data not shown). By 24 h after plating, however, the cells exposed to OXi4503 for 4 h were unable to produce completed tubes at a concentration of 1 μM (Fig. 3b) Treatment with 10 μM *trans*-CA1P for 4 h, though, resulted in tube formation that was not different from controls.

To determine how these agents affected established tube structures, endothelial cells were seeded onto Matrigel and allowed to form tube structures for 18 h prior to drug treatment. When cells were exposed to 10 μM OXi4503 for either 30 min or 4 h, the tubes observed 24 h after treatment showed an almost complete loss of structure (Fig. 4). However, 10 μM *trans*-CA1P did not affect tube structure after either treatment period.

Treatments with either isomer at concentrations up to 10 μM had no effect on either endothelial cell viability, as determined by both trypan blue exclusion or clonogenic cell survival (data not shown), indicating that the functional disruptions observed were not associated with long term cytotoxic effects.

A significant consequence of the vascular collapse initiated in tumors following treatment with VDAs is a loss of perfusion (Holwell et al., 2002; Salmon and Siemann, 2006). In the present study, tumor perfusion in KHT sarcomas was evaluated by diffusion of a gadolinium contrast agent, using DCE-MRI, prior to, as well as 4 and 24 h after, treatment with OXi4503 or *trans*-CA1P (25 mg/kg), using each mouse as its own control. The results (Fig. 5A) showed a decrease in image intensity enhancement after administration of a gadolinium-based contrast agent compared to pre-gadolinium values at various times after drug treatment. As expected, OXi4503 produced a significant decrease in tumor perfusion by 4 h post-treatment. By 24 h post-treatment, perfusion values were lower, but not significantly different from controls. By comparison, there was no significant change in tumor perfusion in mice treated with the *trans*-isomer at either time point evaluated. Representative DCE-MRI images of both groups pre- and post-treatment are shown in Fig. 5B. These data agrees with our previous studies showing that tumor perfusion determined using DCE-MRI correlates with vascular shut-down assessed by Hoechst 33342 staining of patent blood vessels and morphometric determination of tumor necrotic fractions (Salmon and Siemann, 2006; Salmon et al., 2006; Salmon et al., 2007; Siemann, 2010; Wankhede, et al., 2009).

Vascular collapse and reductions in tumor blood flow have been directly linked to subsequent inductions of tumor necrosis and secondary tumor cell death (Salmon at al., 2006). KHT tumors harvested from mice 24 h after treatment with OXi4503 showed a significant dose-dependent decrease in clonogenic cell survival (Fig. 6). In contrast, tumors of mice treated with *trans*-CA1P demonstrated no reduction in clonogenic tumor cell survival. Histological evaluation confirmed the cell survival studies (Fig. 7). While treatment with 25 mg/kg OXi4503 resulted in tumors with a thin viable rim surrounding a necrotic core (Fig. 7c), tumors from mice exposed to the *trans*-isomer (25 mg/kg) were virtually indistinguishable from untreated control tumors (Fig. 7a vs. 7b). The effects on tumor histology of treating mice with a 100 mg/kg dose of CA4P alone (Fig. 7d) or in combination with a 25 mg/kg dose of *trans*-CA1P (Fig. 7e) are shown for comparison. Consistent with previous results (Siemann and Horsman, 2004), KHT sarcomas from mice treated with OXi4503 demonstrated greater extents of necrosis than did those of mice treated with CA4P (Fig. 7c vs. 7d). Most interestingly, the *trans*-isomer of CA1P, which on its own led to no tumor necrosis, markedly reduced the rim of surviving tumor tissue observed following CA4P treatment when administered in conjunction with CA4P (Fig. 7e).

To quantify the extent of necrosis produced by the various treatments, sections from KHT tumors removed 24 h after treatment were assessed using an image analysis system (Rojiani et al., 2002). The results (Fig. 8) showed that whereas both untreated and *trans*-isomer-treated tumors displayed 6-7% necrosis, treatment with 25 mg/kg OXi4503 resulted in ~97% tumor necrosis (Fig. 8). CA4P treatment was less effective (~81% necrosis) than OXi4503 but its impact on tumor histology could be enhanced (~91% necrosis) when combined with *trans*-CA1P.

Discussion

Tubulin-binding-VDAs such as the combretastatins are thought to primarily affect tumor-confined endothelial cells, causing tumor necrosis and secondary neoplastic cell death due to vascular collapse. However, a common observation after treatment with all VDAs is a viable

rim of tumor cells remaining at the periphery, surrounding an area of central necrosis. OXi4503, though, has been shown to yield greater necrosis and a smaller viable rim than other agents in this class of compounds (see Figs. 7-8).

This enhanced efficacy has been ascribed to the generation of oxiquinones, which could yield additional cytotoxic effects in vivo. In addition to vascular disruption via microtubule binding, the formation of reactive orthoquinones that bind to cellular nucleophiles and form free radicals has the potential to directly induce cancer cell death.

Both the *cis*- and *trans*-isomers of CA1P used in this study generate oxiquinones, but only the *cis*-isomer (OXi4503) binds tubulin. As expected, in vivo studies with OXi4503 showed a loss of patent blood vessels and a reduction in tumor perfusion, whereas treatment with the *trans*-isomer did not. Consistent with the in vivo vascular effects, only OXi4503 and not *trans*-CAIP caused endothelial cell tubulin collapse (as observed by immunofluorescence confocal microscopy) and inhibited the formation of tube structures on Matrigel. In addition, OXi4503 exposure also resulted in the collapse of established endothelial cell tubes. Neither isomer showed cytotoxicity in vitro, but this likely is due to the fact that both are phosphorylated and it is the dephosphorylated orthoquinone species that give rise to cytotoxicity (Madlambayan, et al., 2010). In addition, our data are consistent with published studies stating that in vitro functional effects can occur at concentrations far below those that decrease cell viability or proliferation (Bijman, et al., 2006; Schwartz, 2009; Ahmed, et al., 1993).

In keeping with the hypothesis that tubulin-binding-VDAs initiate antitumor effects via their ability to collapse tumor vasculature, the ability of OXi4503 to impair the tumor blood vessel network led to the induction of tumor necrosis and secondary tumor cell death. The *trans*-isomer was unable to do either. Since both isomers are chemically capable of generating a cytotoxic species, these data strongly support the notion that it is the tubulin binding capacity of OXi4503 that is primarily responsible for its antitumor effect. Still, the results of Fig.8 imply that the generation of cytotoxic species may contribute to the overall activity of OXi4503. This conclusion is in keeping with the recent report of apoptotic tumor cells in the viable rim following OXi4503 exposure (B. Pedley, personal communication, 2010) as well as the finding that treatment with this agent could lead to direct cytotoxic effects on leukemia cells in a systemic model of primary human AML (Madlambayan, et al., 2010). However, the present data indicate that the orthoquinone mechanism *per se* is insufficient to be detected by means of cytotoxicity or histological endpoints. Such a finding would not be surprising if the species are generated locally and are short lived as suggested by in vitro investigations. However, the observed ability of the *trans*-isomer to enhance the antitumor efficacy of CA4P, in terms of increased extent of tumor necrosis/reduction in viable tumor rim, strongly implies that the postulated cytotoxic orthoquinone mechanism may, in fact, contribute to the in vivo potency of OXi4503.

Acknowledgments

These studies were supported by a grant from the National Cancer Institute (Public Health Service grant CA084408).

References

Ahmed B, et al. Vascular targeting effect of combretastatin A-4 phosphate dominates the inherent angiogenesis inhibitory activity. Int J Cancer 1993;105:20–25. [PubMed: 12672025]

Azam F, et al. Mechanisms of resistance to antiangiogenesis therapy. Eur J Cancer 2010;46(8):1323–1332. [PubMed: 20236818]

Beerepoot LV, et al. Phase I clinical evaluation of weekly administration of the novel vascular-targeting agent, ZD6126, in patients with solid tumors. J Clin Oncol 2006;24(10):1491–1498. [PubMed: 16574998]

Bijman MNA, et al. Microtubule-targeting agents inhibit angiogenesis at subtoxic concentrations, a process associated with inhibition of Rac1 and Cdc42 activity and changes in the endothelial cytoskeleton. Mo Cancer 2006;5(9):2348–2357.

Bloemendal HJ, et al. New Strategies in anti-vascular cancer therapy. Eur J Clin Invest 1999;29(9): 802–809. [PubMed: 10469169]

Calligaris D, et al. Microtubule targeting agents: from biophysics to proteomics. Cell Mol Life Sci 2010;67(7):1089–1104. [PubMed: 20107862]

Chan LS, et al. Selective targeting of the tumour vasculature. ANZ J Surg 2008a;78(11):955–967. [PubMed: 18959693]

Chan LS, et al. Alterations in vascular architecture and permeability following OXi4503 treatment. Anticancer Drugs 2008b;19(1):17–22. [PubMed: 18043126]

Chan LS, et al. Effect of vascular targeting agent Oxi4503 on tumor cell kinetics in a mouse model of colorectal liver metastasis. Anticancer Res 2007;4B:2317–2323. [PubMed: 17695520]

Chaplin DJ, et al. Current development status of small-molecule vascular disrupting agents. Curr Opin Investig Drugs 2006;6:22–528.

Davis PD, et al. ZD6126: a novel vascular-targeting agent that causes selective destruction of tumor vasculature. Cancer Res 2002;62(24):7247–7253. [PubMed: 12499266]

Denekamp J. Endothelial cell proliferation as a novel approach to targeting tumour therapy. Br J Cancer 1982;45:136–139. [PubMed: 7059456]

Denekamp J. The tumour microcirculation as a target in cancer therapy: a clearer perspective. Eu J Clin Invest 1999;29(9):733–736.

Denekamp J, Hobson B. Endothelial-cell proliferation in experimental tumours. Br J Cancer 1982;46:711–720. [PubMed: 7171453]

Dowlati A, et al. A phase I pharmacokinetic and translational study of the novel vascular targeting agent combretastatin a-4 phosphate on a single-dose intravenous schedule in patients with advanced cancer. Cancer Res 2002;62(12):3408–3416. [PubMed: 12067983]

Folkes LK, et al. Oxidative metabolism of combretastatin A-1 produces quinone intermediates with the potential to bind to nucleophiles and to enhance oxidative stress via free radicals. Chem Res Toxicol 2007;20(12):1885–1894. [PubMed: 17941699]

Gaya AM, Rustin GJ. Vascular disrupting agents: a new class of drug in cancer therapy. Clin Oncol (R Coll Radiol) 2005;17(4):277–290. [PubMed: 15997924]

Galbraith SM, et al. Effects of combretastatin A4 phosphate on endothelial cell morphology in vitro and relationship to tumour vascular targeting activity in vivo. Anticancer Res 2001;21(1A):93–102. [PubMed: 11299795]

Grosios K, et al. In vivo and in vitro evaluation of combretastatin A-4 and its sodium phosphate prodrug. Br J Cancer 1999;81(8):1318–1327. [PubMed: 10604728]

Hamel E, Lin CM. Interactions of combretastatin, a new plant-derived antimitotic agent, with tubulin. Biochem Pharmacol 1983;32(24):3864–3867. [PubMed: 6661259]

Hansen S, et al. The prognostic value of angiogenesis by Chalkley counting in a confirmatory study design on 836 breast cancer patients. Clin Cancer Res 2000;6:139–146. [PubMed: 10656442]

Hill SA, et al. Preclinical evaluation of the antitumour activity of the novel vascular targeting agent Oxi 4503. Anticancer Res 2002;22(3):1453–1458. [PubMed: 12168822]

Hobson B, Denekamp J. Endothelial proliferation in tumours and normal tissues: continuous labelling studies. Br J Cancer 1984;49:405–413. [PubMed: 6201181]

Holwell SE, et al. Combretastatin A-1 phosphate a novel tubulin-binding agent with in vivo anti vascular effects in experimental tumours. Anticancer Res 2002;22(2A):707–711. [PubMed: 12017147]

Horsman MR, Siemann DW. Pathophysiologic effects of vascular-targeting agents and the implications for combination with conventional therapies. Cancer Res 2006;66(24):11520–39. [PubMed: 17178843]

Hua J, et al. Oxi4503, a novel vascular targeting agent: effects on blood flow and antitumor activity in comparison to combretastatin A-4 phosphate. Anticancer Res 2003;23(2B):1433–1440. [PubMed: 12820406]

Kallman RF, et al. Factors influencing the quantitative estimation of the in vivo survival of cells from solid tumors. J Natl Cancer Inst 1967;39(3):539–549. [PubMed: 6053718]

Kanthou C, Tozer GM. Microtubule depolymerizing vascular disrupting agents: novel therapeutic agents for oncology and other pathologies. Int J Exp Pathol 2009;90(3):284–294. [PubMed: 19563611]

Kirwan IG, et al. Comparative preclinical pharmacokinetic and metabolic studies of the combretastatin prodrugs combretastatin A4 phosphate and A1 phosphate. Clin Cancer Res 2004;10(4):1446–1453. [PubMed: 14977848]

Ljungkvist AS, et al. Vascular architecture, hypoxia, and proliferation in first-generation xenografts of human head-and-neck squamous cell carcinomas. Int J Radiat Oncol Biol Phys 2002;54(1):215–228. [PubMed: 12182995]

Lin CM, et al. Interactions of tubulin with potent natural and synthetic analogs of the antimitotic agent combretastatin: a structure-activity study. Mol Pharmacol 1988;34(2):200–208. [PubMed: 3412321]

Lippert JW 3rd. Vascular disrupting agents. Bioorg Med Chem 2007;15(2):605–15. Epub 2006. [PubMed: 17070061]

Madlambayan GJ, et al. Leukemia regression by vascular disruption and anti-angiogenic therapy. Blood. 2010 Epub May 14 ahead of print.

Malcontenti-Wilson C, et al. Combretastatin A4 prodrug study of effect on the growth and the microvasculature of colorectal liver metastases in a murine model. Clin Cancer Res 2001;7(4):1052–1060. [PubMed: 11309357]

McKeage MJ, Baguley BC. Disrupting established tumor blood vessels: an emerging therapeutic strategy for cancer. Cancer 2010;116(8):1859–1871. [PubMed: 20166210]

Rojiani, AM.; Rojiani, MV. Morphologic manifestations of vascular-disrupting agents in preclinical models. In: Siemann, DW., editor. Vascular-targeted therapies in oncology. Wiley; London: 2006. p. 81-84.

Rojiani AM, et al. Activity of the vascular targeting agent combretastatin A-4 disodium phosphate in a xenograft model of AIDS-associated Kaposi's sarcoma. Acta Oncol 2002;41(1):98–105. [PubMed: 11990526]

Rossi A, et al. Angiogenesis inhibitors and vascular disrupting agents in non-small cell lung cancer. Curr Med Chem 2009;16(30):3919–3930. [PubMed: 19747132]

Rustin GJ, et al. Phase I clinical trial of weekly combretastatin A4 phosphate: clinical and pharmacokinetic results. J Clin Oncol 2003;21(15):2815–2822. [PubMed: 12807934]

Salmon HW, Siemann DW. Effect of the second-generation vascular disrupting agent OXi4503 on tumor vascularity. Clin Cancer Res 2006;12(13):4090–4094. [PubMed: 16818709]

Salmon HW, et al. Evaluations of vascular disrupting agents CA4P and OXi4503 in renal cell carcinoma (Caki-1) using a silicon based microvascular casting technique. Eur J Cancer 2006;42(17):3073–3078. [PubMed: 16956760]

Salmon BA, Siemann DW. Characterizing the tumor response to CA4P treatment. Int J Radiat Oncol Biol Phys 2007;68:211–217. [PubMed: 17448875]

Salmon BA, et al. Monitoring the treatment efficacy of the vascular disrupting agent CA4P. Eur J Cancer 2007;43:1622–1629. [PubMed: 17451938]

Sheng Y, et al. Combretastatin family member OXI4503 induces tumor vascular collapse through the induction of endothelial apoptosis. Int J Cancer 2004;111(4):604–610. [PubMed: 15239140]

Shnyder SD, et al. Combretastatin A-1 phosphate potentiates the antitumour activity of cisplatin in a murine adenocarcinoma model. Anticancer Res 2003;23(2B):1619–1623. [PubMed: 12820431]

Siemann DW, Horsman MR. Targeting the tumor vasculature: a strategy to improve radiation therapy. Expert Rev Anticancer Ther 2004;4(2):321–327. [PubMed: 15056061]

Siemann DW, Horsman MR. Vascular targeted therapies in oncology. Cell Tissue Res 2009;335(1):241–248. [PubMed: 18752004]

Siemann DW, et al. Differentiation and definition of vascular-targeted therapies. Clin Cancer Res 2005;11(2 Pt 1):416–420. [PubMed: 15701823]

Siemann DW, et al. Vascular targeting agents enhance chemotherapeutic agent activities in solid tumor therapy. Int J Cancer 2002a;99(1):1–6. [PubMed: 11948484]

Siemann DW, Rojiani AM. Enhancement of radiation therapy by the novel vascular targeting agent ZD6126. Int J Radiat Oncol Biol Phys 2002b;53:164–171. [PubMed: 12007956]

Siemann DW, Rojiani AM. The vascular disrupting agent ZD6126 shows increased antitumor efficacy and enhanced radiation response in large advanced tumors. Int J Radiat Oncol Biol Phys 2005;62:846–853. [PubMed: 15936569]

Siemann DW, et al. A review and update of the current status of the vasculature-disabling agent combretastatin-A4 phosphate (CA4P). Expert Opin Investig Drugs 2009;18(2):189–197.

Siemann DW, et al. Vascular-targeting therapies for treatment of malignant disease. Cancer 2004;100(12):2491–2499. [PubMed: 15197790]

Siemann DW. The unique characteristics of tumor vasculature and preclinical evidence for its selective disruption by Tumor-Vascular Disrupting Agents. Cancer Treat Rev. 2010 epub Jun. 4.

Schwartz EL. Antivascular actions of microtubule-binding drugs. Clin Cancer Res 2009;15(8):2594–2601. [PubMed: 19351751]

Sriram M, et al. Design, synthesis and biological evaluation of dihydronaphthalene and benzosuberene analogs of the combretastatins as inhibitors of tubulin polymerization in cancer chemotherapy. Bioorg Med Chem 2008;16(17):8161–8171. [PubMed: 18722127]

Thorpe PE. Vascular targeting agents as cancer therapeutics. Clin Cancer Res 2004;10(2):415–427. [PubMed: 14760060]

Vincent L. Combretastatin A4 phosphate induces rapid regression of tumor neovessels and growth through interference with vascular endothelial-cadherin signaling. J Clin Invest 2005;115(11):2992–3006. [PubMed: 16224539]

Wankhede, M., et al. In vivo functional differences in microvascular response of 4T1 and Caki-1 tumors after treatment with OXi4503. 2009.

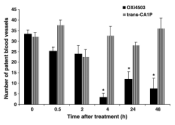

Fig. 1.

Patent tumor blood vessels. KHT sarcoma-bearing mice were treated with 25 mg/kg of either OXi4503 (*cis*-isomer of CA1P) or *trans*-CA1P. Tumors were harvested and patent blood vessels quantified based on Hoechst 33342 staining at various times after drug exposure. *, $p<0.001$ versus controls.

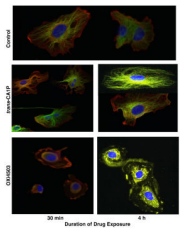

Fig. 2.

Effect of OXi4503 and *trans*-CA1P on microtubule assembly in human microvascular endothelial cells (HMVEC-L). Cells were exposed to 5 or 10 μM of the appropriate isomer for either 30 min or 4 h, then fixed and immunostained with antibodies to β-actin (Cy3, red) and β-tubulin (Cy2, green), with overlaid red-green areas appearing yellow. Nuclear DNA was counterstained with DAPI (blue). Representative confocal fluorescent color-merged images are shown here. Merged Magnification: 100×.

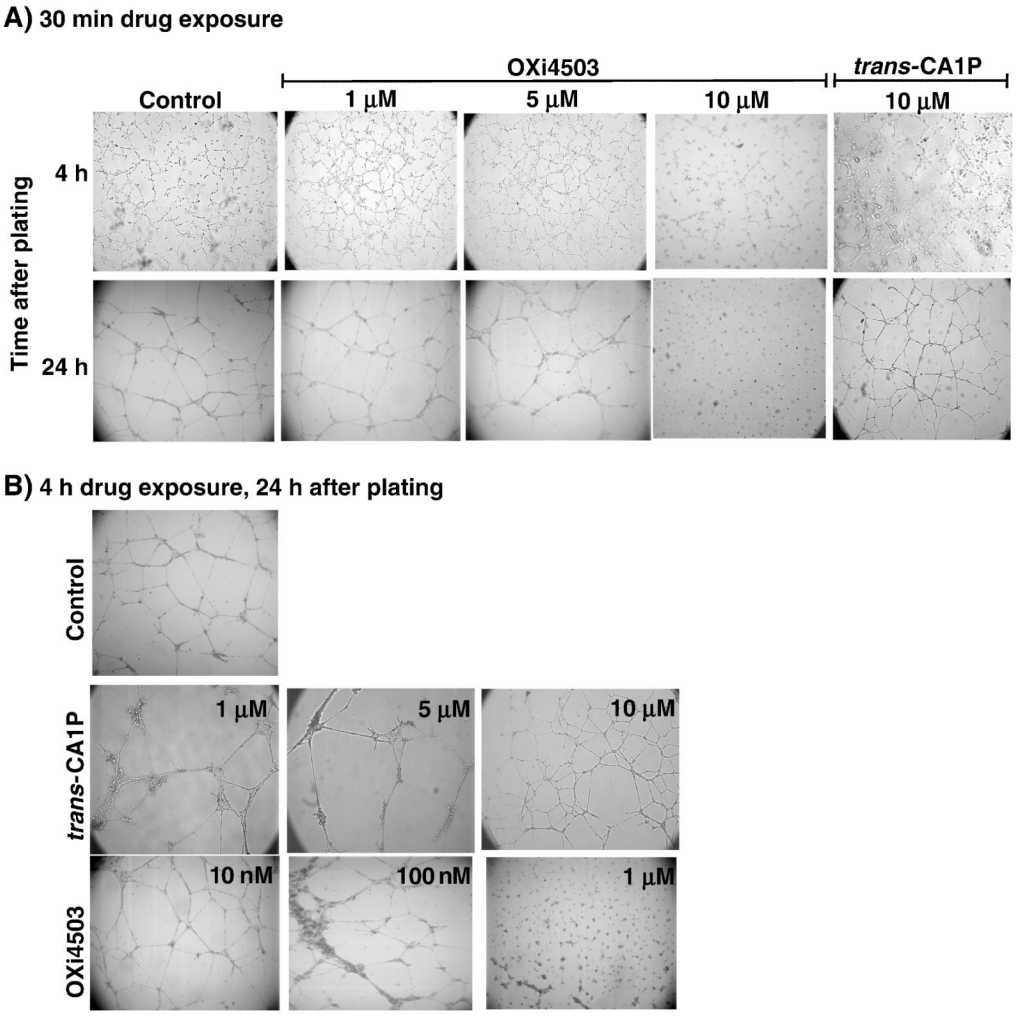

Fig. 3.

Effect of OXi4503 and *trans*-CA1P treatment on the ability of human microvascular endothelial cells (HMVEC-L) to form tubes. Cells were exposed to various concentrations of the appropriate isomer for 30 min and assessed at 4 h or 24 h post-plating (a) or treated for 4 h prior to plating on Matrigel® and assessed at 24 h post-plating (b).

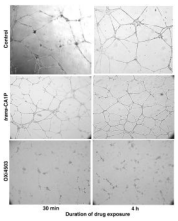

Fig. 4.

Effect of OXi4503 and *trans*-CA1P treatment on established endothelial cell (HMVEC-L) tubes. Cells were plated on Matrigel® and allowed to form tubes for 18 h, then exposed to 10 μM concentrations of the appropriate isomer for 30 min or 4 h. Tube status was assessed 24 h post-treatment.

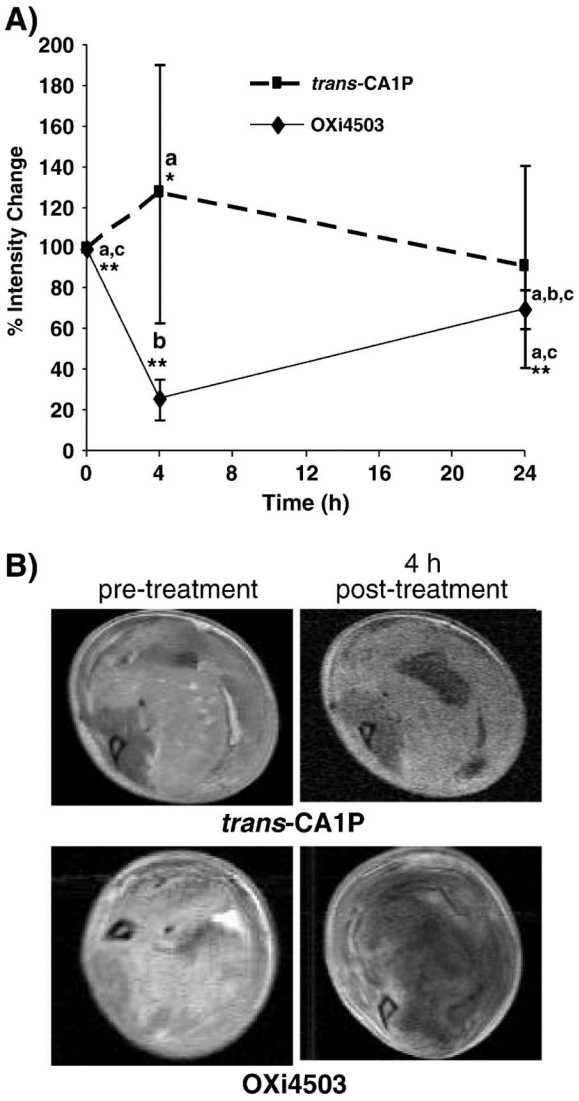

Fig. 5.

Effect of OXi4503 and *trans*-CA1P (25 mg/kg) on tumor perfusion in mice bearing KHT tumors. (a) The percent change in signal enhancement of the tumor area due to diffusion of a gadolinium contrast agent was measured prior to, and 4 and 24 h after treatment with either *trans*-CA1P or OXi4503, from an average of at least 4 mice per group, ± SEM. Each mouse was used as its own control. Data points with different letters are significantly different from each other. *, p=0.02; **, p=0.0001. (b) Representative DCE-MR images of KHT tumors prior to treatment and again 4 h after treatment with either *trans*-CA1P or OXi4503. Images show bright areas of gadolinium diffusion. Necrotic areas remained dark. At 4 h post-treatment, tumors in mice treated with OXi4503 underwent vascular collapse and extensive tissue damage, as evidenced by the lack of gadolinium signal enhancement beyond the tumor rim.

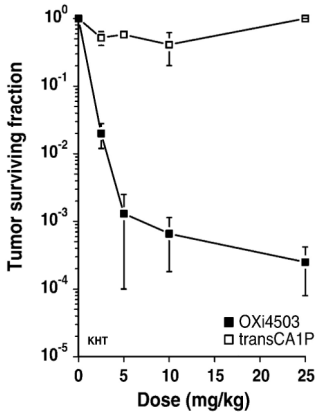

Fig. 6.

Clonogenic cell survival of KHT sarcoma cells. Mice bearing intramuscular KHT sarcomas were treated with a range of doses of either OXi4503 or *trans*-CA1P. Tumor cell survival was determined 24 h post-treatment. Data shown are the mean ± SEM of 3 experiments.

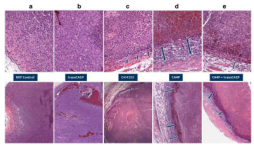

Fig. 7.

Tumor histology. Representative H&E-stained tissue sections of intramuscular KHT sarcomas of mice that were untreated (a) or treated with 25 mg/kg *trans*-CA1P (b) or OXi4503 (c), 100 mg/kg CA4P (d), or 25 mg/kg *trans*-CA1P plus 100 mg/kg CA4P (e). Tumors were harvested 24 h post-treatment. Top panels, magnification: 20×. Bottom panels, magnification: 10×. Arrows indicate areas of viable neoplastic tissue at the edge of the tumors.

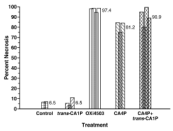

Fig. 8.

Percent tumor necrosis. KHT sarcoma-bearing mice were kept as controls or treated as described in Fig. 7. Twenty-four h post-drug exposure, tissue sections were prepared and percent necrosis assessed by image analysis (Methods section). Data represent individual tumors; for each tumor 3-4 sections were evaluated.